Fluid Flow Velocity Measurement in Active Wells Using Fiber Optic Distributed Acoustic Sensors

Nafiseh Vahabi, *Member, IEEE*, Eero Willman, Hadi Baghsiahi and David R.Selviah, *Member, IEEE*

***Abstract*—Real time monitoring of the behaviour of fluids along the whole length of fluid filled well pipes is important to the oil and gas industry as it enables well operators to maximize oil and gas production and optimize the quality of oil and gas produced, whilst reducing the cost. Flow speed measurement is one of the key approaches in fluid flow monitoring in wells. In this paper, three methods are designed, developed and demonstrated to estimate the speed and direction of flow at a range of depths in real world oil, gas and water wells using acoustic data set from distributed acoustic sensors that attached to the wells. The developed methods are based on a new combination of several techniques from signal processing, machine learning and physics. The Terabyte size acoustic dataset are recorded from each well as a two-dimensional function of both distance along the pipeline and time. The aim of the developed methods is estimating flow speed at each point along over 3000 meters pipelines and increasing the accurately and efficiently of the flow speed calculation compared to the existing method. The methods developed in this paper are computationally inexpensive, which make them suitable for real time well monitoring.**

***Index Terms*—Fluid characterization, fluid flow measurement, flow velocity, Hough transform, K-means clustering, optical sensors,**

I. Introduction

THE instrumentation for real time condition monitoring of the behaviour of fluids along the whole length of well pipes and boreholes is of critical importance for oil and gas production energy industry. Monitoring of such oil production wells can detect when the flow from an almost depleted oil reservoir is also bringing out sand that contaminates the flow and must be removed at the surface, which is a costly process. If sand is detected then the flow can be throttled down to control the system and the sand will then fall back and not emerge at the surface [1]. There are two main type of flow measurements devices for well pipes, single-point measurement and multiple-point measurement. Single-point measurement devices measure fluid flow speeds and temperatures at just one point along the pipe. For example, ultrasonic sensors [2], [3] can be used to detect the size and number of gas bubbles within the fluid [4] and to determine the flow velocity profile in a cross section of the pipe [5]. Point measurement Digital Coriolis Mass Flow Meters can also measure the flow of a two phase fluid in real time making use of Field Programmable Gate Array (FPGA) which are advantageous for real time control optimisation [6]. Other point flow meters include Electrical Capacitance Tomography for visualisation of solid contaminants in a gas pipeline [7], [8] and Kinematic Wave point detection [9]. The major disadvantage of the single-point measurement devices is providing measurement only at one point [10]. Also, they have to be installed prior to the pipe insertion.

Multiple-point measurement devices such as Distributed Temperature Sensor (DTS) [11], [12] monitor the temperature along the whole length of the pipeline with clear advantages over the single-point measurement techniques. Distributed Acoustic Sensor (DAS) is one the most recently developed flow measurement tool that records the acoustic sounds and vibrations along the whole length of well pipeline [2], [13], [14]. DAS systems use optical fibres which attach to the main fluid filled pipeline [15]–[17] to monitor acoustic sounds and vibrations. The iDAS, developed by Silixa [18] is an optoelectronic system which records the true acoustic signal continuously along the path of a sensing optical fiber tens of kilometers long [19]–[21]. The iDAS has a frequency range from millihertz to hundreds of kilohertz. Sounds and vibrations are generated from different sources such as turbulent fluid flow, sand in the fluid scraping along the side of the pipe, the sea waves at the surface and unauthorised tampering on a pipeline.

The aim of this paper is to develop the algorithms to extract from acoustic signals an estimation of the fluid flow speed. Only some of the many sounds recorded within the well are useful for extraction of the flow speed so this paper develops and optimises a combination of signal processing algorithms to filter out unwanted sounds and keep wanted sounds which enable the fluid flow speed to be calculated.

The rest of this paper is organized as follows. Section II outlines the DAS dataset used in this study. The mechanism of DAS system to record acoustic signals is described in Section III. In Section IV, the pre-processing techniques are presented. Three proposed flow estimation methods are presented in Section V. The results of our methods are described in Section VII. Section VIII discusses our finding in details. Finally, Section IX concludes this paper.

II. Dataset

The algorithms were tested on three sets of data which were collected from an oil, water and gas wells. The sensing fiber

Manuscript received Month xx, 2xxx; revised Month xx, xxxx; accepted Month x, xxxx. This work was supported in part by the xxx Department of xxx under Grant (sponsor and financial support acknowledgement goes here).

N. Vahabi and David R. Selviah are with the Department of Electronic and Electrical Engineering, University College London, London, UK, e-mail: (Nafiseh.Vahabi.14@ucl.ac.uk).

E. Willman is a Principal Software Developer and H. Baghsiahi is a Quality Assurance Engineer at Correvate Limited, UK.

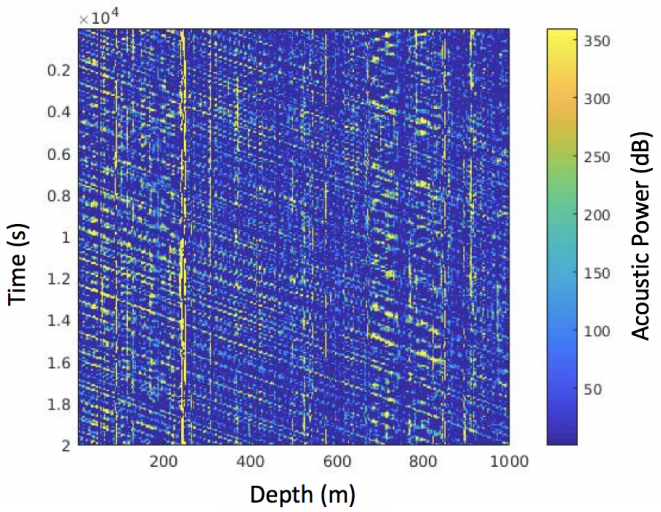

Fig. 1: Sample of visualized raw signals. This data was collected by a distributed acoustic sensor in distance and time from a water pipe. The data is mapped to the color range $[0, 350]$ to enhance visualization.

cable was $4235\ m$ long strapped to the production tubing and data is collected with 10 kHz temporal frequency. Table I provides the details of each pipeline such as the length of the optical fiber for each pipe [22]. The Packer True Vertical Depth is the vertical distance from a final depth to a point at the surface which is usually less than the optical fiber length. The other parameters of the pipes such as their diameter and pipe material are not considered in this study nor the acoustic wave guide properties of the well bore. Raw data is illustrated in Fig. 1 with time on the vertical axis and depth of the measurement on horizontal axis. In Fig. 1 X-shaped cross lines can be seen, due to sound waves traveling up and down in the fluid inside the pipe.

TABLE I: THE PROPERTIES OF PIPES

Well Type	Packer True Vertical Depth (m)	Length Optical (m)
Oil well	2600	3000
Gas well	2700	3500
Water well	2400	3200

III. Mechanism of recording acoustic data by DAS

Distributed Acoustic sensor (DAS) is composed by an optoelectronic unit and optical fibre cable. An optoelectronic unit is located at the surface of the sea [15], [19].The optical fibre is run down a well alongside a pipe carrying a fluid and it is attached to that pipe at the points with a meter apart. Optical fibers are thin flexible cables consisting of glass (silica) threads that are capable of transmitting light waves. DAS measurement begins by sending a laser pulse down the optical fibre from the optoelectronic unit. The traveling light within the fiber backscatters from non- uniformities in the glass at each point along the optical fiber [16]. As the fluid mixture travels through the pipe its motion is very turbulent and it generates a noisy sound. The acoustic waves propagate through the fluid in the well pipes in the direction of fluid flow and also against the fluid flow direction. Acoustic waves exert a dynamic pressure on the well pipe and it causes local changes in the well pipe's radial strain. DAS can capture all these local strains at each point attached to the pipe because as acoustic waves travel through the fluid, their pressure fluctuation can be picked up at each attached point along DAS with some time delay. Backscattered lights encounter changes caused by flow acoustic waves when traveling through the line and it goes to Optical Time-Domain Reflectometer (OTDR) that is connected to the end of the fiber optic line in optoelectronic unit [20]. OTDR is used to test for breaks and backscattering points in optical fiber telecommunication fibers. A pulse of light is sent into the fiber, reflects from some discontinuity or slight change in refractive index and returns to the OTDR. The delay shows how far along the fiber the reflection point is found. Many such reflection points can be found in this way. A broadband light source is used to avoid coherent backscatter interference, which is sometimes referred to as Coherent Rayleigh Noise. However, instead of avoiding it, it can instead be used by detecting the fast changes in the coherent backscatter Rayleigh signal [23]. The Silixa distributed acoustic sensor [24] extends this idea to measure the acoustic signal (amplitude, frequency and phase) and so calculate axial strain changes at all points along the optical fiber.

The optoelectronic unit measures all the axial strain changes occur through the optical fibre. DAS works by measuring the pressure changes at each point along the fibre and builds a dynamic profile of those changes and hence, it is capable to measure the acoustic field. Therefore, the optoelectronic unit records both phase and amplitudes of the acoustic signals at each point that optical fibre attached to the well pipe [17], [19]. The sound is recorded continuously at each attached point of optical fibre cable to the well pipe and this results in an enormous amount of data recorded each day [19]. Data collected by DAS contains the acoustic power in decibels (dB) information stored in thousands of files. Each data file typically contains one minute of acoustic dataset. Therefore, each acoustic data file contains the information about the time the fluctuation is captured and the known distance between sensors. This is the most advantageous characteristic of DAS for monitoring wellbore because it enables the analysis of fluid flow at each point along the well pipe that is attached to DAS.

Acoustic waves exert a dynamic pressure on the well pipe and it causes local changes in the well pipe's radial strain. DAS can capture all these local strains at each point attached to the pipe because as acoustic waves travel through the fluid, their pressure fluctuation can be picked up at each attached point along DAS with some time delay. Therefore each acoustic data file contains the information about the time the fluctuation is captured and the known distance between sensors. This is the most advantageous characteristic of DAS for monitoring wellbore because it enables the analysis of fluid flow at each point along the well pipe that is attached to DAS.

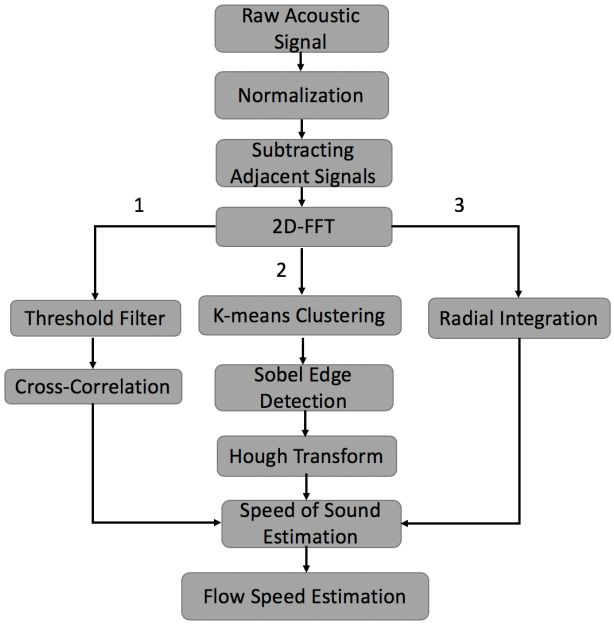

Fig. 2: Flow speed estimation methods. The flowchart shows each step of three approaches to estimate the speed of sound and ultimately the flow speed at each point along the well pipe.

IV. Pre-processing acoustic data

In this study the raw data is pre-processed and the speed of sound is estimated by designing three novel approach as demonstrated in Fig. 2. We subtracted the acoustic signals recorded from adjacent effective sensor positions to filter out unwanted strong noise sounds and keep wanted sounds which enable the fluid flow speed to be calculated. These unwanted sounds originate from sound sources external to the well pipe, typically from other nearby wells. The sounds from a point source some distance away will arrive at two adjacent sensors at about the same time so by subtracting signals for adjacent sensors we can remove these external sounds. Having measured the speed of sound by three methods, we will consider the Doppler Effect [22] and calculate the flow velocity. The details of each technique are presented in section V. A summary of the main findings are reported in the results section, which compares the speed of flow versus depth calculated by each method.

A. Time versus distance normalization

As some parts of the optical fibre DAS are tightly bound to the fluid filled pipe they will record a higher amplitude acoustic signal so it is advantageous to first perform a normalisation along the depth or distance axis of the data to make all the amplitudes the same. The average amplitude at each depth can be found by calculation of the standard deviation or variance along the time axis [25]. Then this can be normalised along the depth axis. In our recent study on this dataset [26], four normalization techniques were implemented and it has been reported that statistical normalization is the most suitable one for our dataset. Therefore, acoustic signals were normalized as a function of time at different depths along the fiber.

B. 2D Fast Fourier Transform

Two dimensional Fast Fourier transform is applied to convert dataset from time domain to frequency domain [27], where k, f and $G(k, f)$ represent the wave-number, frequency and DAS signal of the sample data respectively.

$$G(k,f) = \int\int f(x,t)e^{-j(kx-2\pi ft)}\,\mathrm{dxdt} \tag{1}$$

2D-FFT is capable of revealing aspects of data that are not easily detected in the time-space domain like trends, discontinuities, and self-similarity. In order to increase the performance of the 2D-FFT algorithm, we should transform the height and width of an image to an integer power of two [28]. Hence, 2D-FFT is applied with a moving window of 256 samples in distance and $16,384$ samples in time. 256 samples in distance are chosen to maintain a good number of spatial frequency bins [29]. $16,384$ samples in time are chosen because of the sampling rate in time is 10 kHz and $16,384$ is the closest power of 2 number which is not sampling lower than the Nyquist frequency [30]. The result, $G(k, f)$, contains a pair of V-shaped lines which are used to predict the speed of the propagating acoustic wave. Fig. 3 shows the result of applying a two dimensional Fast Fourier Transform on 2D representations. As it seen in Fig. 3 (a) the data in the frequency versus wave-number domain forms a V-shape and the slope of its arms determines speed of the sound in fluid flow according to:

$$\nu = \frac{2\pi f}{k} \tag{2}$$

If the slope of the fitted lines to the arms of the V-shape is positive we can conclude the sound is traveling upward in the pipe, otherwise the sound is traveling down the well pipe. Hence, from now on we concentrate on the methods which can extract as many of the pixels from the V-shape line for further analysis. The result of the 2D FFT is normalized with respect to the frequency and the wave number which are shown in Fig. 3 (b) and Fig. 3 (c) respectively. The outcome of the wave number normalization (Fig. 3 (c)) enhances the brightness of the V-shape compared with the original V-shape (Fig. 3 (a)) and the outcome of the frequency normalization (Fig. 3 (b)) [31]. Therefore, the wave number normalization outcome is selected as the input for the next method which is the hard threshold. The threshold is defined as $\lambda = \sqrt{2\log_{10} p}$ according to the hard threshold definition [32] where p is the mean of the pixel's intensity. All the pixels below the threshold are set to zero as shown in Fig. 3:

$$G(k,f) = \begin{cases} G(k,f) & G(k,f) \geq \lambda \\ 0 & G(k,f) < \lambda \end{cases} \tag{3}$$

The threshold is defined as the top 0.2% of the sample amplitude. The thresholded image is formed of the set of pixels which are mostly extracted from the V-shape lines as it shown in Fig. 4 (a).

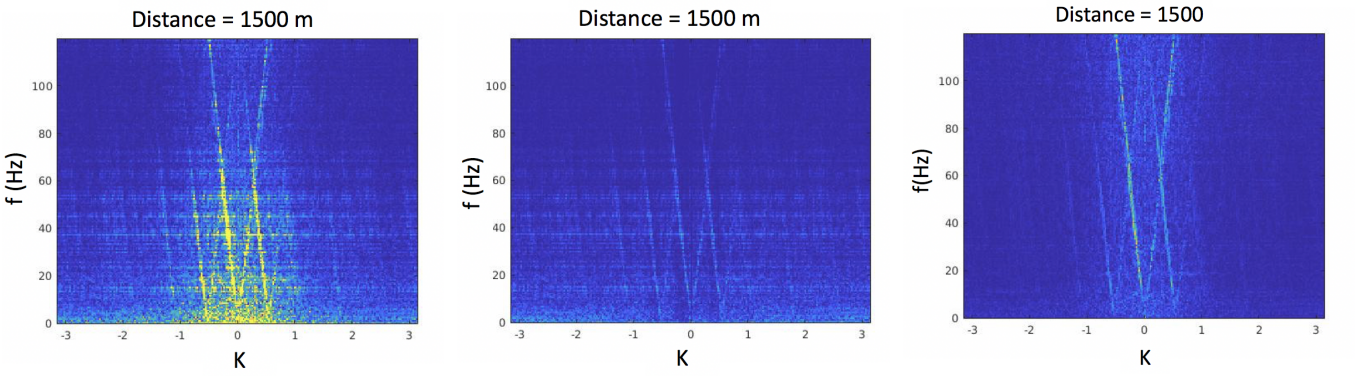

(a) 2D FFT (b) Normalized 2D FFT with frequency (f) (c) Normalized 2D FFT with wave number (k)

Fig. 3: 2D FFT and k versus f normalization- The results of applying 2D FFT to acoustic signals are presented in the two dimensional (a). The result was normalized with regards to the frequency (b) and the wave number (c). However, normalizing the frequency spreads the noise out along the x-axis whilst normalizing the wave number results in the clear V-shape.

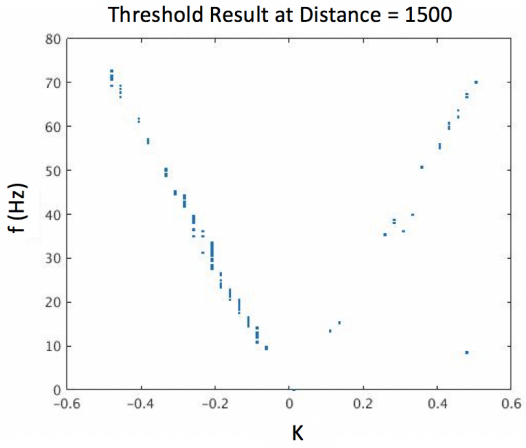

Fig. 4: The result of applying a threshold filter on the 2D FFT image.

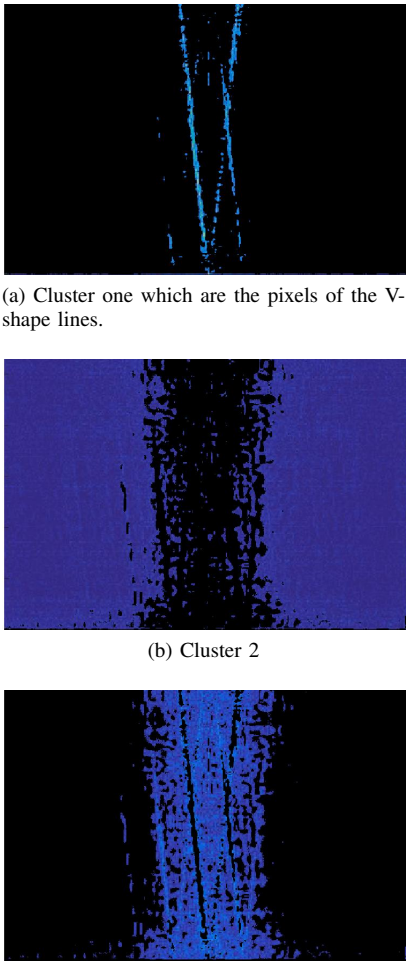

(a) Cluster one which are the pixels of the V-shape lines.

(b) Cluster 2

(c) Cluster 3

Fig. 5: K-means clustering result. The algorithm extracts the points of V-shape lines. $k-f$ plot for water flow data from at depth = $1000\ m$. Two linear features are corresponding to the speed of sound propagating up or down the well.

V. Algorithms to Estimate the Speed of Sound

The following three sections will investigate three methods to estimate the speed of sound.

A. Method one: Cross correlation

In the first flow speed estimation approach (Fig. 2), the outcome of 2D-FFT is fed into threshold filter and then Cross-correlation method. Cross-correlation is an operation to measure the similarity between two signals at different time lag positions [34]. By using cross correlation between acoustic signals at different positions along the fiber, the time shift of the wave between the different positions can be calculated [35], [36]. If $u(t)$ and $v(t)$ are two acoustic signals along the fiber, t and τ represent time and the integration variable respectively. $d(t)$ is the time lag between two signals, $u(t)$ and $v(t)$, and can be obtained from Eq. 4.

$$d(t) = u(t) \otimes v(t) = \int_{-\infty}^{+\infty} u^*(\tau - t)v(\tau)\mathrm{d}\tau \qquad (4)$$

The details of the mathematical derivation can be found in [34], [37].

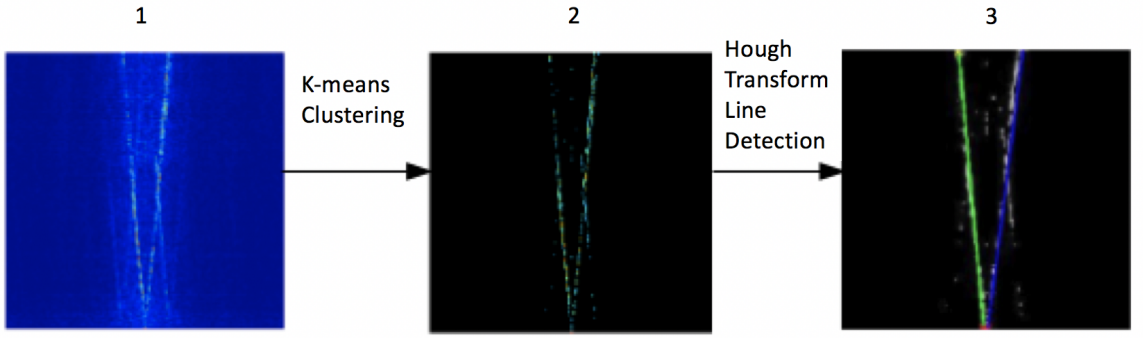

Fig. 6: Hough Transform line detection algorithm detects the two lines in the V-shape cluster (step 2). The image in step 3 shows the superimposed green and purple lines on the pixels of the V-shape image.

B. Method two: K-means Clustering and Hough transform line detection

In the second flow speed estimation approach (Fig. 2), K-means clustering is implemented for extraction of informative signals. K-means clustering is a classification algorithm that divides data into K clusters depending on their attributes where K is a positive integer number [38]. Initially, K objects are selected randomly as the seed objects and the other objects assigned to each seed based on their distance to each seed. In each iteration the centroid of each cluster is calculated and the objects move to the group which is closest to its centroid. The iteration process will stop when there are no more objects to move into the new cluster [39]. We tried few numbers ($K = 2, 3, 4, 5, 6$) to initialize the K-means clustering algorithm. For the number of cluster more than 4 algorithm was stuck in a local minimum and it did not converge. For $K = 2, 3, 4$ the algorithm converged successfully and $K = 3$ yielded the lower sum of squared distance therefore, we selected 3 clusters.

The K-means clustering method is implemented by using the normalized V-shaped data (Fig. 3 (c)) to extract the group of pixels forming the V-shape [40]. The image data is clustered into three groups based on the Euclidean distance metric. As shown in Fig. 5 (a), one of the clusters is clearly a V-shape which is fed into a line detection algorithm called Hough Transform. The details of mathematical derivation can be found in [39].

The Hough Transform technique has a common application in image processing when it is required to define some features of a shape in a parametric form. The main advantage of the Hough Transform technique which makes it suitable for our application is its gap tolerance in feature boundary descriptions. In addition, it is capable of identifying features automatically and the result is not affected by the image noise [41]. The Hough Transform algorithm takes the V-shape cluster as an input and detects the lines in the image. Image 3 in Fig. 6 shows the green line (left arm) and the purple line (right arm) were detected by the Hough Transform algorithm which were superimposed on the V-shape cluster image (Fig. 6, image 2). The slope of the detected lines is used for the speed of sound calculation.

C. Method three: Radial Integration Algorithm

The Third flow speed estimation (Fig. 2) approach is an integration along a radius in a polar diagram that is superimposed at the f versus k origin. The integration can be summarized as a summation of data values organized on a discrete grid along lines or rays emanating at different angles, θ, from a predetermined point (in case of continuous representation of data, the data would be integrated along the lines instead of summing). For each considered angle θ, the summed value, E, is divided by the number of pixels that formed the line for normalization and is stored in a one-dimensional list or array. Upon plotting E vs. θ (Fig. 7 (c)), distinct peaks become visible for angles θ that coincide with the orientation of any linear features passing through the point of interest. This reduces the problem complexity from detecting lines and their orientations on a 2D grid to detection of peaks positions on a 1D signal. All lines emanating from the origin of the f versus k plot and extending to each pixel location along the left, right and top edges of the plot are considered. Essentially, this traces the rectangular external boundary of the Fig. 7 (a) shows the original image and the white lines are superimposed on the V-shape (Fig. 7 (b)) signal lines. The energy function can be seen in Fig. 7 (c) which shows two peaks in the graph indicating the two lines of the V-shape image Fig. 5 (a).

VI. Flow speed estimation

We use the speed of sound estimation from three developed methods to estimate flow speed. Due to the Doppler Effect, the speed of sound traveling along the flow direction will appear faster, and the flow speed can be determined by

$$v = \frac{\nu_1 - \nu_2}{2} \tag{5}$$

where v is speed of flow, ν_1 and ν_2 are speed of sound traveling along and opposite to the flow direction respectively.

VII. Results

The results of three developed methods to analyse oil, water and gas dataset are presented in Fig. 8. The dataset is collected from each well during 2×10^4 s and along over 3000 m well pipe which is a very large dataset. we consider block of data over the time and distance in our analysis. The flow speed

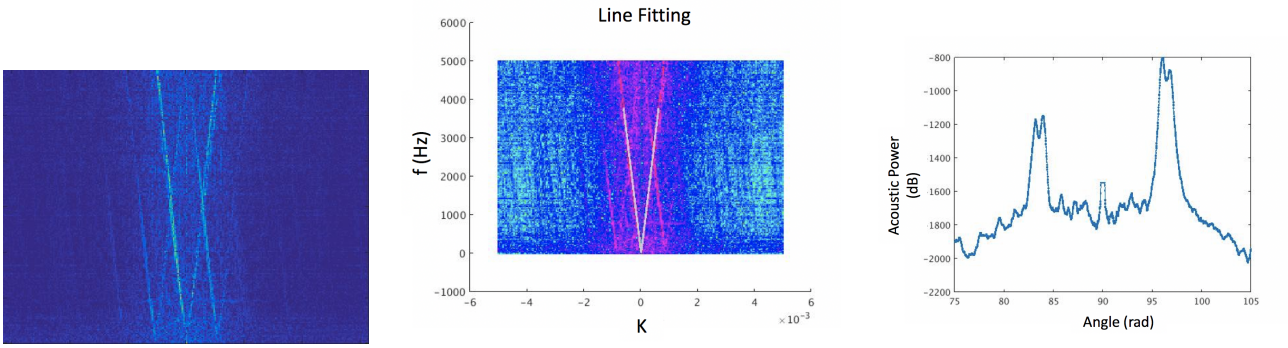

(a) The signal after applying 2D FFT. (b) The line found by radial integration function superimposed on the original image. (c) Energy function which is summation of pixels through integration.

Fig. 7: Two linear features passed through the origin, each corresponding to the speed of sound propagating up or down the well.

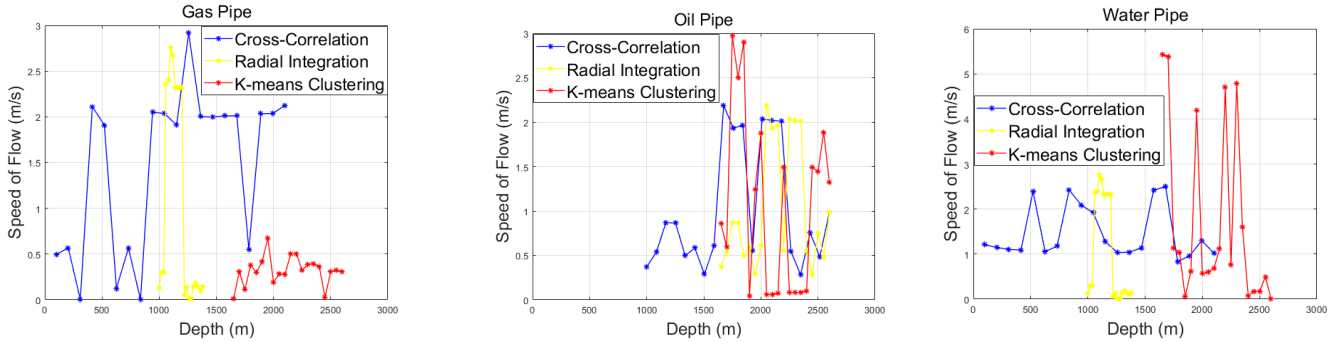

(a) Gas Well (b) Oil Well (c) Water Well

Fig. 8: The result of implementing three methods to estimate the flow speed in gas (a), oil (b) and water (c) showed in these diagrams.

does not change in the same location at different time stamp. However, the flow speed changes at different depth along the well pipe due to changes in a flow pressure. In most cases, a file containing one minute of acoustic data could not be loaded with available computing resources. To overcome the challenge of handling large data files, we divided the raw data into a series of blocks for processing. The size of the block depends on the desired spatial and temporal resolution for calculated velocity profiles. For the next block, the window was moved by a time samples and half of spatial samples. Halving the spatial window size is performed to enhance repeatability and to increase spatial resolution in the results [19]. The end result is a set of $k - f$ plots overlapping in distance and covering the entire file content as shown in Fig. 7 (a).

The type of fluid in each pipe is different and has different properties. As it seen in Fig. 8, each method only performs on certain depth of the well pipe. In water and gas pipes, Cross-Correlation estimation is between 100 m and 2200 m, Radial integration is between 1000 m and 1400 m and K-means clustering is between 1700 m and 2700 m (Fig. 8 (a) (c)). However, for the oil pipe, Cross-correlation estimates the flow speed between 1000 m and 2600 m and the other two algorithms perform well between 1700 m and 2600 m (Fig. 8 (b)). Amongst all the algorithms, the Cross-Correlation can provide a flow speed estimation on the longest part of the pipe which is 2000 m, however the K-means clustering method is the only one which is capable of extracting the signals between 2100 m and 2700 m and estimating the flow speed.

In gas and water wells, the results (Fig. 8 (a), (c)) are shown the Cross-Correlation performs well in shallower (less than 1000 m) and K-means Clustering method performs in deeper (more than 2000 m) depths of the well pipes. In oil well, none of the methods provide a flow speed estimation in shallower area as it shown in Fig. 8 (b). Also, the Cross-Correlation estimation is consistent and agrees with K-means clustering and the Radial integration estimation results in the middle depth (between 1000 m and 2000 m). Table II summarises the result of the three approaches and compares them with the estimation from flow meter which locates at the well head. It should be noted that the result of the three approaches are the mean of flow estimation all along each pipe but flow meter estimation is just at one point which is well head at the surface of the sea.

When considering table II, we see that for the oil well Cross Correlation and Radial Integration are closest to the well head

TABLE II: COMPARING MEAN OF ESTIMATED FLOW SPEED

Well Type	Cross Correlation (m/s)	K-means Clustering (m/s)	Radial Integration (m/s)	Flow Meter at Well Head (m/s)
Oil Well	1.6362	0.3339	3.0362	2.8000
Gas Well	1.2691	1.5915	0.2457	6.9600
Water Well	1.4558	2.0718	2.4329	2.1000

flow meter with Radial Integration being the closest. For the Gas well Cross Correlation and K-means clustering are the closest but some way off from the well head flow meter. In the water well, K-means clustering is the closest with the other two methods about a half metre per second different one higher and one lower.

VIII. DISCUSSION

Radial integration and K-means clustering methods use Doppler shift for flow estimation which means they require detection of acoustic waves travelling both up and down the well to enable both sides of the V-shape in the frequency versus wave-number plot to be detected. We found that there were only certain regions in the well where this occurred, typically when there were sources of sound above and below the measurement point or places where sound waves travelling down the pipe could be reflected back up the pipe and vice versa. In other places along the well only one side of the V-shape would be detected so any calculations based on Doppler shift would give very poor results. However, we found that in many of these cases the Cross-Correlation method worked very well as it did not depend on having two sides to the V-shape.

Table II averages across all the results in Fig. 8 and so hides a lot of the detail giving deceptive results. A number of the data points in Fig. 8 could reasonably be excluded from the average. If it known that these well pipes did not have side branches bringing in or removing additional flow then we would expect the flow speed to remain approximately constant and not fluctuate wildly from one location to a nearby location along the pipe.

In the Gas well, the very low values of flow speed for Radial integration occur when the V shape in the frequency versus wave-number did not have one of the sides of the V. So by detecting that the V-shape did not have one of its sides, these low readings can be excluded. The issue with detecting one arm of the V-shape is also valid for all of the K-means clustering results. Similarly, the sudden changes in Cross-correlation flow speed from 2 to 0 m/s are not physically reasonable and so the low values of the Cross-correlation flow speed can be excluded. Therefore we conclude that the results within about 1 m/s of 2 m/s can be kept and that then there is good agreement between Cross-correlation and Radial integration and giving an average flow speed of approximately 2.2 m/s less than the 6.96 m/s well head flow meter.

In the water well, there is similar reasoning. We can keep the flow speed values within a range of 0.5 m/s of the maximum and minimum Cross-correlation flow speed results giving an average of the remaining points of about 1.4 m/s which is less than the 2.1 m/s well head flow meter. In the Oil well, there are large fluctuations of flow speed over very short distances along the well which are not physically reasonable. Here we know that Cross-correlation is robust against difficulty in detecting the two sides of the V-shape in the frequency versus wave-number plots. So preserving flow speeds within 1 m/s of the 2 m/s Cross-correlation flow speeds enables us to exclude all of the very slow flow speeds. Now we make an interesting observation that when the K-means clustering is not working properly giving very low flow speeds, the Radial integration is working very well and vice versa. The average of these points gives a flow speed of approximately 2.1 m/s less than the 2.8 m/s of the well head flow meter.

The well head flow-meter measures volume flowing per second from which the speed is inferred. It is not surprising that the calculated results are all less than the well head flow speeds as the fluids at deeper depth are under high pressure which is relieved as they approach the surface resulting in a larger volume flow speeds and that the largest difference is for gas which compresses the most with pressure. It was expected that the actual flow speed would differ from the well head volume flow meter.

IX. CONCLUSION

We conclude that the Cross-correlation is the most reliable method for flow speed estimation using DAS dataset. However, it was advantageous to average it together with the K-means clustering and radial integration results within a small range around the cross-correlation results. We also note that in the oil well K-means clustering and radial integration are complementary techniques yielding results when the other technique is not reliable, so these should be combined together. In addition, there is a stronger complementary effect in the gas and water pipes where radial integration gives results at lower depths and K-means clustering gives results at deeper depths. It is clear that if there is too much background noise in the frequency versus wave-number plots, radial integration will lead to erroneous results while K-means clustering has the ability to extract the signal from the noise across the frequency versus wave-number plots. Radial integration method works very well when the background noise is very low. Detection of the background noise level (Fig. 7 (c)) can be used to determine whether Radial integration is likely to be unreliable. If sources of sound could be deliberately introduced along the well to reliably generate downward travelling and upward travelling sound waves then the K-means clustering

and radial integration methods would operate reliably over a longer length of the well. Sound sources can be introduced by including partially open in-flow control valves and other types of constriction to increase turbulence of flow.

REFERENCES

[1] Chaudhuri, A., Sinha, D.N., Zalte, A., Pereyra, E., Webb, C. and Gonzalez, M. E., " Mass Fraction Measurements in Controlled Oil-Water Flows Using Noninvasive Ultrasonic Sensors," *Journal of Fluids Engineering*, vol.3, 2014.

[2] Gysling, Daniel L., and Mark R. Myers, "Distributed sound speed measurements for multiphase flow measurement", U.S. Patent 6,601,458, issued August 5, 2003.

[3] Gysling, Daniel L, "Fluid density measurement in pipes using acoustic pressures", U.S. Patent 6,971,259, issued December 6, 2005.

[4] Goh, C. L., Ruzairi, A., R., Hafiz, F., R. and Tee, Z., C., "Simulative and Experimental Studies: Void Fraction Detection in a Bubble Column of a Conducting Pipe", *IEEE Transactions on Industrial Electronics*, vol.64, no.12, pp.9636–9645, 2017.

[5] Ricci, S., Meacci, V., Birkhofer, B. and Wiklund, J., "FPGA-based system for in-line measurement of velocity profiles of fluids in industrial pipe flow", *IEEE Transactions on Industrial Electronics*, vol.64, no.5, pp.3997–4005, 2017.

[6] Shawash, J. and Selviah, D., R., "Real-time nonlinear parameter estimation using the Levenberg–Marquardt algorithm on field programmable gate arrays", *IEEE Transactions on Industrial Electronics*, vol.60, no.1, pp.170–176, 2013.

[7] Meribout, M. and Saied, I., M., "Real-time two-dimensional imaging of solid contaminants in gas pipelines using an electrical capacitance tomography system", *IEEE Transactions on Industrial Electronics*, vol.64, no.5, pp.3989–3996, 2017.

[8] Ismail, I., Gamio, J. C., Bukhari, S. A., and Yang, W. Q., "Tomography for multi-phase flow measurement in the oil industry," *Flow Measurement and Instrumentation Journal*, vol.16, pp.145–155, 2005.

[9] Lucas, G. P., and I. C. Walton, "Flow rate measurement by kinematic wave detection in vertically upward, bubbly two-phase flows," *Flow Measurement and Instrumentation Journal*, vol.8, pp.133–143, 1998.

[10] Chong, C. Y. and Kumar, S. P. , "Sensor networks: evolution, opportunities, and challenges," *Proceedings of the IEEE*, vol.37, no.1, pp.1247–1256, 2003.

[11] Smolen, J. J. and Van der Spek, A., "Distributed Temperature Sensing", A DTS Primer for Oil & Gas Production," *EP2003*, vol.5, 2003.

[12] Brown, G. A. and others"Monitoring multilayered reservoir pressures and GOR changes over time using permanently installed distributed temperature measurements," *SPE Annual Technical Conference and Exhibition*, 2006.

[13] Finfer, D. C., Mahue, V., Shatalin, S., Parker, T. and Farhadiroushan, M., "Borehole Flow Monitoring using a Non-intrusive Passive Distributed Acoustic Sensing (DAS)," *SPE Annual Technical Conference and Exhibition*, 2014.

[14] Li, M., Wang, H., Tao, G., "Current and future applications of distributed acoustic sensing as a new reservoir geophysics tool," *The Open Petroleum Engineering Journal*, vol.8, no.1, 2015.

[15] Baldwin, C. S., "Applications for fiber optic sensing in the upstream oil and gas industry," *International Society for Optics and Photonics*, vol.9480, pp.194800D, 2015.

[16] Hicke, K., Hussels, M. T., Eisermann, R., Chruscicki, S and Krebber, K., "Condition monitoring of industrial infrastructures using distributed fibre optic acoustic sensors," *Optical Fiber Sensors Conference (OFS), 2017 25th*, pp.1–4, 2017.

[17] He, X., Pan, Y., You, H., Lu, Z., Gu, L., Liu, F., Yi, D. and Zhang, M., "Fibre optic seismic sensor for down-well monitoring in the oil industry," *Measurement*, vol.123, pp.145–149, 2018.

[18] Silixa's granted UK patents on the iDAS and flow monitoring methods. GB2482641, GB2517100 and GB251732 all Farhadiroushan, Parker and Shatalin.

[19] Xiao, J., Farhadiroushan, M., Clarke, A., Abdalmohsen, R. A., Alyan, E., Parker, T. R. and Milne, H. C., "Intelligent Distributed Acoustic Sensing for In-well Monitoring," *In SPE Saudi Arabia Section Technical Symposium and Exhibition*, Society of Petroleum Engineers, 2014.

[20] Raman, C., "A new radiation," *Indian Journal of Physics*, vol. 2, pp. 387–398. 1928.

[21] Chen, V. C., Li, F., Ho, S-S and Wechsler, H.,"Micro-Doppler effect in radar: phenomenon, model, and simulation study," *IEEE Transactions on Aerospace and electronic systems*, vol.42, no.1, pp. 2–21, 2006.

[22] Johannessen, K., Drakeley, B. K. and Farhadiroushan, M., "Distributed Acoustic Sensing-a new way of listening to your well/reservoir," *In SPE Intelligent Energy International*, Society of Petroleum Engineers, 2012.

[23] Shatalin, S.V., Treschikov, V.N. and Rogers, A.J., "Interferometric optical time-domain reflectometry for distributed optical-fiber sensing," *Applied optics*, vol.37, no.24, pp. 5600–5604, 1998.

[24] Farhadiroushan, M., Parker, T.R. and Shatalin, S.," Method and apparatus for optical sensing," WO2010136810A2, 2009.

[25] Russo, F., "An image enhancement technique combining sharpening and noise reduction," *Instrumentation and Measurement, IEEE Transactions on*, vol.51, no.4, pp.824–828, 2002.

[26] Vahabi, N., Alabdullah, M. and Selviah, D. R., "Acoustic Sensors to Measure Speed of Oil Flow in Downhole Pipes," *14th IEEE Conference on Industrial Electronics and Applications (ICIEA)*, pp.2411–2416, 2019.

[27] Rioul, O. and Flandrin, P., "Time-scale energy distributions: a general class extending wavelet transforms," *IEEE Transactions on Signal Processing*, vol.40, no.7, pp.1746–1757, 1992.

[28] Ervin S., Igor D. and LJubiÅ¡a S., "Fractional Fourier transform as a signal processing tool: An overview of recent developments," *IEEE Signal Processing Magazine*, vol.91, no.6, pp.1351–1369, 2011.

[29] Park, C. S., "2D Discrete Fourier Transform on Sliding Windows," *IEEE Transactions on Image Processing*, vol.24, no.3, pp.901–907, 2015.

[30] Tao, R., Li, Y. L. and Wang, Y., "Short-Time Fractional Fourier Transform and Its Applications," *IEEE Transactions on Signal Processing*, vol.58, no.5, pp.2568–2580, 2010.

[31] Shie Q., and Dapang C., "Joint time-frequency analysis," *IEEE Signal Processing Magazine*, vol.16, no.2, pp.52–67, 1999.

[32] Rami, C., "Signal Denoising Using Wavelets," Israel Institute of Technology, Department of Electrical Engineering, http://tx.technion.ac.il/ rc, 2012

[33] O'Rourke, J., "An on-line algorithm for fitting straight lines between data ranges," *Communications of the ACM*, pp.574–578, 1981.

[34] Lewis, J. P., "Fast normalized cross-correlation," *In Vision interface*, vol.10, no.1, pp.120–123, 1995.

[35] Nikias, C. L. and Mendel, J. M., "Signal processing with higher-order spectra," *IEEE Signal Processing Magazine*, vol.10, no.3, pp.10–37, 1993.

[36] Krim, H. and Viberg, M., "Two decades of array signal processing research: the parametric approach," *IEEE Signal Processing Magazine*, vol.13, no.4, 67–94, 1996.

[37] Knapp, C. H. and Carter, G. C., "The generalized correlation method for estimation of time delay," *Acoustics, Speech and Signal Processing, IEEE Transactions on*, vol.24, no.4, 320–327, 1976.

[38] Teknomo, K., "K-means clustering tutorial," *Medicine*, vol.100, no.4, pp.3, 2006.

[39] Jain, A. K., "Data clustering: 50 years beyond K-means," *Pattern recognition letters*, vol.31, no.8, pp.651–666, 2010.

[40] Chen, C., Luo J. and Parker, K. J., "Image segmentation via adaptive K-means clustering and knowledge-based morphological operations with biomedical applications," *IEEE Transactions on Image Processing*, vol.7, no.12, pp.1673–1683, 1998.

[41] Chen, Y., Li, Y., Zhang, H., Tong, L., Cao, Y. and Xue, Z., "Automatic power line extraction from high resolution remote sensing imagery based on an improved Radon transform," *Pattern Recognition*, vol.49, pp.174–186, 2016.

[42] Li, Z., Jing, L. and Murch, R., "Propagation of monopole source excited acoustic waves in a cylindrical high-density polyethylene pipeline," *The Journal of the Acoustical Society of America*, vol.142, pp.3564–3579, 2017.

ACKNOWLEDGMENT

The authors thank Statoil and Silixa for permitting the use of the iDAS data acquired as part of a multiple well field trial campaign for the data analysis described in this paper. The authors thank the UK Government for funding via the Technology Strategy Board, TSB, Project Number 100722, Distributed Acoustic Flow Meter, with project partners Chevron, Statoil, Saudi Aramco, Silixa, UCL and Weatherford. The author Nafiseh Vahabi also thanks the UK Government Research council EPSRC for funding her research.

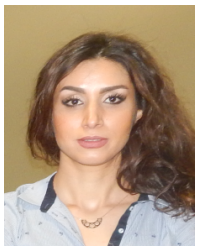

Nafiseh Vahabi (S'11- M'15) received her MEng degree in Computer Science with Artificial Intelligence from Electronics and Computer Engineering department at University of Southampton, UK, in 2013. Then, she joined Imperial College London, UK, and received her master degree (MRes) in Medical Robotics and Image Guided Intervention in 2014. Nafiseh was awarded the scholarship from Engineering and Physical Science Research Council (EPSRC) to pursue her PhD in Electronic and Electrical Engineering Department at University College London where she awarded her PhD in 2019.

She was awarded an EPSRC Doctoral Prize Fellowship to develop deep learning algorithms to analyze Electrical Impedance Tomography dataset from premature neonates lung. She is currently a research fellow in Sensors, System and Circuit research group within Electronic and Electrical Engineering Department, UCL. Her research interest is machine learning, deep learning, image processing and signal processing.

Dr Vahabi is a member of Institute of Engineering and Technology, member of IEEE and IEEE Woman in Engineering. She is an Associate Fellow of Higher Education Academy.

Eero Willman received his MEng and PhD degrees in Electronic Engineering from University College London in 2003 and 2009 respectively. After that he worked as a post doctoral research associate at University College London until 2014 and currently he is employed as a Principal Software Developer at Correvate Limited, in the UK. His main areas of interest include development of numerical algorithms, finite elements analysis and image and signal processing algorithms.

Hadi Baghsiah received his Bachelor and Master degree in Iran in Physics and optical engineering and finished his PhD degree in University College London in 2012 on design and developing high data rate Optical printed circuit boards. His main research areas include optical system design and evaluation, Optical waveguide, polymer waveguide, signal processing, distributed acoustic sensors for oil and gas industry and extra resolution optical microscopy. He is also involved in 3D printing, 3D laser scanning, image processing in his research activities.

David R.Selviah (M'01) born in England, UK. He received the BA degree and MA degree in physics and theoretical physics in 1980 and 1984 respectively and the PhD degree in photonic engineering in 2009 from Trinity College, Cambridge University, Cambridge. UK.

He served internships at the Royal Aircraft Establishment, UK, Texas Instruments, UK and CERN, Switzerland. From 1980 to 1983, he was with the Allen Clark Research Center, Plessey (Caswell) Ltd., UK (now Oclaro). From 1983-1986, he was with the Department of Engineering Science, Oxford University, UK. He is currently a Reader in Optical Devices, Interconnects, Algorithms and Systems in the Optical Devices and Systems Laboratory of the Photonics Research Group in the Electronic and Electrical Engineering Department at University College London, London, UCL. He serves as a consultant for UCL and VorteQ Consulting. He is the author of many published articles, keynote presentations and patents. His research is generally carried out in collaboration with international companies and universities. His current research interests include multimode polymer optical waveguides, fibers and connectors for high bit rate communication in data centers, dispersion in single and multimode optical fibers, silicon photonic DFB lasers, signal processing, image processing, pattern recognition, big data analysis, cloud computing, 3D Lidar and photogrammetry, 3D track classification, stimulation and monitoring neural behavior, data analysis for distributed acoustic sensors in oil and gas wells. http://www.ee.ucl.ac.uk/staff/academic/dselviah.

Dr Selviah is a member of the Institute of Physics, Optical Society of America, European Optical Society and is a Chartered Physicist and Chartered Scientist. He represents the UK on the International Electrotechnical Commission Standards committees IEC TC86, SC86 WG4, SC86 WG6 and JWG9 covering optical fiber connectors, attenuation measurement techniques and optical circuit boards.